SVC CONTROL DESIGN CONCEPTS FOR SYSTEM DYNAMIC PERFORMANCE

INVITED PAPER FOR IEEE SPECIAL SYMPOSIUM ON APPLICATION OF STATIC VAR SYSTEMS FOR SYSTEM DYNAMIC PERFORMANCE

E.V. Larsen, Sr. Member, IEEE J.H. Chow, Sr. Member, IEEE
General Electric Company
Schenectady, NY 12345

1. INTRODUCTION

The electric power industry now has considerable experience with Static VAR Compensators (SVC's). Many have been installed for high-voltage transmission system enhancement around the world since the 1970's, and much has been written about application considerations, including several books [1-8].

The contribution of this paper is to provide insights to two basic aspects of SVC applications: voltage regulator stability, and the use of SVC's to aid damping of power system swings. It is hoped that these insights will provide helpful guidelines for quantifying the potential improvement of the dynamic performance of power systems that can be obtained from an SVC.

Voltage regulation is the primary mode of control for most SVC's. The transient response of this control mode is important to overall system performance, but there exists a limit to the speed of response. This limit is determined by the tendency of the voltage regulation loop to become lightly damped, with the potential for spontaneous growth of oscillations - typically above 20 Hz. The underlying causes of this behavior are presented in this paper, along with curves providing representative constraints on maximum voltage-regulator gain. These representative constraints should be helpful in selecting appropriate voltage-regulator settings for planning studies. Special control enhancements are possible to improve stability margins, should this be required in certain applications.

Application of SVC's to provide an important addition to damping of power swings is of increasing interest. This paper presents a discussion of the basic system characteristics which are important for the appropriate application of the SVC for damping.

Many of the results presented in this paper are from a current EPRI-sponsored research project (RP2707-1). Additional results, obtained as this project is completed, will be available in the final report.

2. SVC CONTROL STRUCTURE

The basic SVC control structure is illustrated in Figure 2.1. Several variations on this basic structure exist, but this structure contains the essential features needed to explain the concepts presented in this paper.

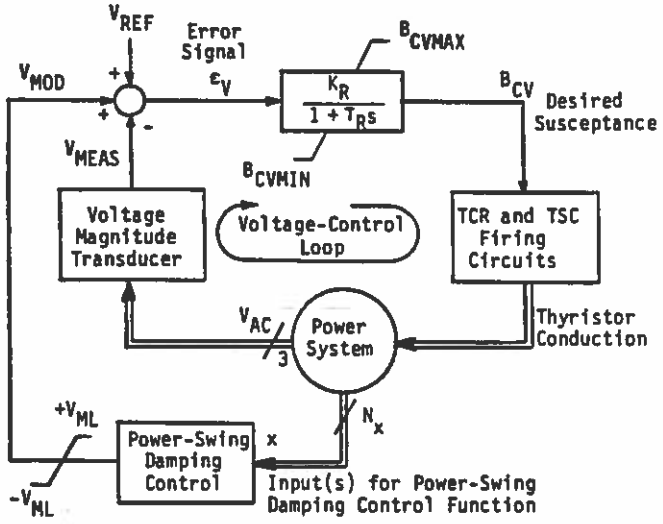

Figure 2.1 Basic SVC Control Structure, Including Illustration of Closed Loops via Power System.

The output of the regulator B_{CV} is the desired susceptance of the controllable portion of the SVC. The firing circuits typically include a nonlinearity to convert the desired susceptance value to a firing-angle command for the TCR. This nonlinearity is based upon the known relationship between the effective TCR susceptance B_T and firing angle σ_T. In practice, this nonlinear function is often implemented in an approximate manner, such as with a series of straight-line segments; however, this approximation has little influence on the overall SVC behavior discussed in this paper. In TCR/TSC types, the firing logic also coordinates the TCR and TSC to smoothly achieve the desired net B_{CV}.

The primary control function is performed by a voltage regulator, consisting of a gain and a time-constant. The gain K_R establishes the steady-state droop characteristics of the SVC. A typical value for K_R is approximately 20 pu/pu, yielding full response for a 5% voltage error. The combination of the gain K_R and the time constant T_R establishes the speed of response to a given error signal. A special term is defined here to represent the speed of response, called the "transient gain":

$$K_T = K_R / T_R \quad \text{(pu/sec/pu)} \qquad (2.1)$$

where

K_T = "Transient gain" = rate of SVC response to 1.0 pu error.

K_R = Gain of voltage regulator, expressed in per unit on total controllable admittance (i.e., $B_{CVMAX} - B_{CVMIN}$) change for 1.0 per unit voltage error.

T_R = Time constant of voltage regulator.

Typical values for the time constant range from 50 to 300 milliseconds, yielding transient gain values of from 67 pu/sec/pu to 400 pu/sec/pu.

The voltage-regulating loop is closed by sensing an ac voltage, typically at the high voltage bus of the SVC. This three-phase set of alternating voltages is input to a transducer which creates a direct signal proportional to the magnitude of the positive-sequence voltage phasor. Several techniques may be used in such a transducer, but all result in performance characteristics similar to those discussed in this paper.

The power-swing damping function is included as a modulation function on the voltage regulator.

3. VOLTAGE REGULATION STABILITY

The voltage-regulating loop of an SVC can, under certain circumstances, become unstable. Such an instability is characterized by growing oscillations in the regulator signals, the frequency of which is typically in excess of 20 Hz. An example is shown in Figure 3.1, where spontaneous growth of 20 Hz oscillations are evident in the measured voltage-magnitude signal and in the regulator output signal. Note that the actual ac voltage and TCR current signals are amplitude-modulated with the 20 Hz oscillations.

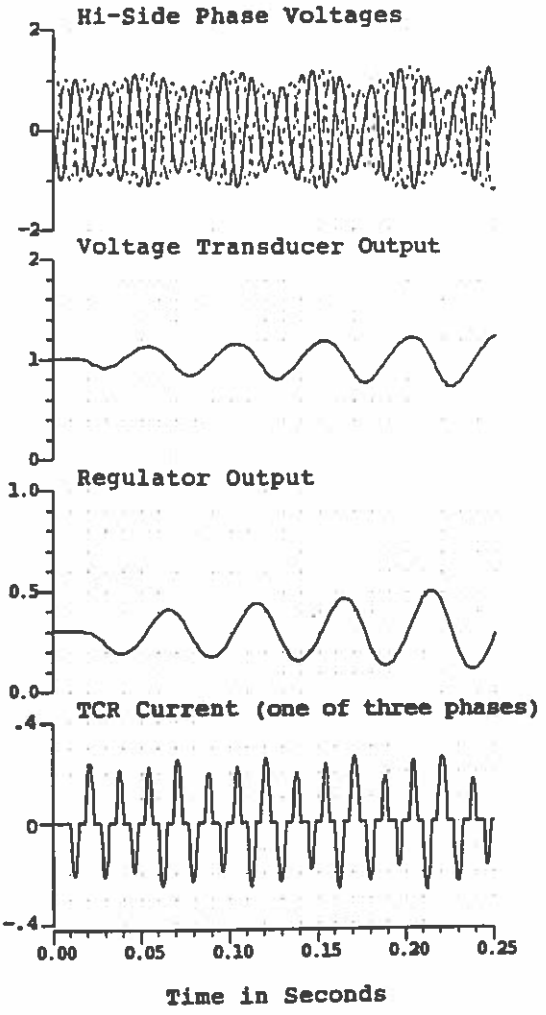

Figure 3.1 Example of SVC Voltage - Control Instability.

This section describes the basic power system parameters which influence the stability margin of the SVC voltage-regulating loop, and provides representative limits on transient gain as a function of these system parameters.

3.1 Important Power System Parameters

The strength of the power system, as viewed from the SVC, is an important factor in the voltage-regulating loop gain. The strength determines the amount of ac voltage change due to a change in SVC reactive current.

Of equal importance in the limiting cases is the dynamic response of the power system. The resonance characteristic of the power network creates an effective time delay between SVC control action and a change in ac voltage magnitude. When added to the delay of the voltage regulator and the inherent delays associated with firing of the TCR's, a total phase lag of 180° can occur at a frequency much lower than would be expected solely from the control elements. An instability will then occur if the loop gain is too high. The instability illustrated in Figure 3.1 results because the system has 180° total phase lag at approximately 20 Hz, thus producing 20 Hz oscillations with excessive amplitude.

To quantify the relationships of these characteristics to voltage-regulation stability, two power system parameters must be defined. The parameters chosen relate to the total power system as viewed from the TCR portion of the SVC; thereby including all filters and capacitors, plus the transformer of the SVC. Figure 3.2 provides an example impedance versus frequency characteristic for an SVC application.

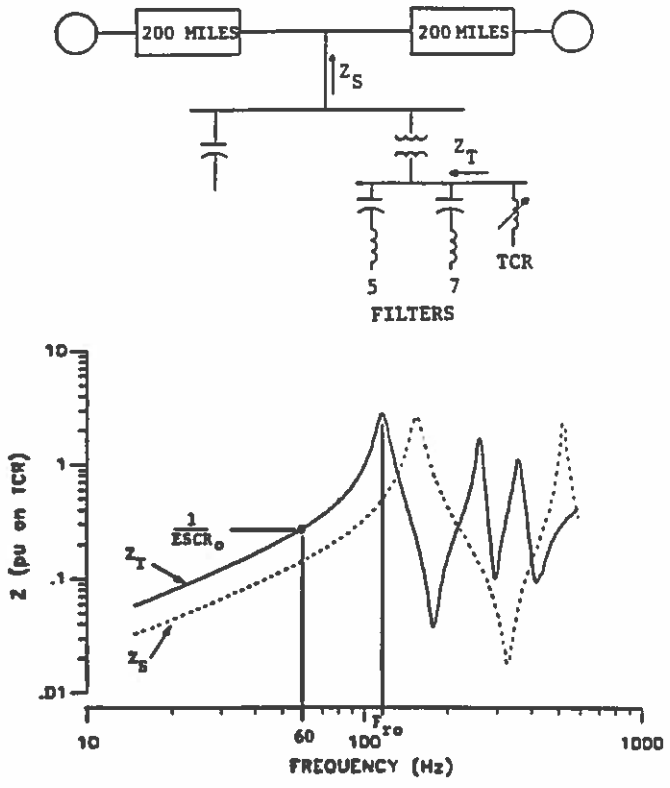

Figure 3.2 Example of Impedance -vs- Frequency Characteristic in SVC Application.

The key parameters selected for ac-system definition are:

1. $ESCR_o$ = Effective Short-Circuit Ratio, expressed in per unit on the full-conduction admittance of the TCR.

2. F_{ro} = First-Resonant frequency of the ac system, including all filters and capacitors of the SVC, and the SVC transformer.

$ESCR_o$ is a measure of the driving-point impedance of the power system at fundamental frequency, as viewed from the TCR, which is important to the steady-state gain of the voltage-control loop.

F_{ro} is a measure of the natural transient response of the power system, which is important to the dynamic characteristics of the voltage-control loop.

Note that both the $ESCR_o$ and F_{ro} parameters defined above will be lower than the corresponding quantities for the ac system existing prior to adding the SVC, due to the capacitors and transformer of the SVC. These quantities can be obtained from a frequency-scanning type of impedance calculation program, and should be determined for both nominal system conditions and extreme contingencies for which SVC stability is important.

A general trend exists for practical power systems whereby strength implies a first-resonant frequency being within a certain range. An example is illustrated in Figure 3.3 for an SVC application midway between major load or generation areas. (All lines leaving the SVC bus are of approximately equal length and are equivalenced as a single line with surge-impedance loading (SIL) equal to the sum of all lines.) Note that for a given ESCR, F_r varies with the amount of shunt compensation; however, the general trend is for the resonant frequency to decrease as the system becomes weaker.

3.2 Sensitivity to Power System Parameters

Figure 3.4 illustrates the effect of power system parameters on the transient response of the voltage-regulating loop, for various voltage-regulator settings. Results from twelve different cases are shown in this figure, with the voltage-transducer feedback and regulator-output signals provided for each case. Three power system configurations are represented, from a weak system ($ESCR_o$ = 0.7 pu, F_{ro} = 80 Hz) to a strong system ($ESCR_o$ = 2.5 pu, F_{ro} = 180 Hz). Four regulator settings are represented, from very fast (K_T = 1000 pu/sec/pu) to sluggish (K_T = 30 pu/sec/pu). Each case consists of a three-phase fault applied at 50 msec, cleared at 100 msec.

The general trends of the effect of power system strength on stability margin are clear in Figure 3.4.

The importance of the power system resonance is illustrated in Figure 3.5, which compares the transfer function from regulator output to ac voltage magnitude for power systems having two different resonant frequencies (80 Hz and 110 Hz). These two cases also have different $ESCR_o$ levels, resulting in different steady-state gains (-2.5 db versus -6.2 db at very low modulation frequency). However, the influence of low power-system resonant frequency is apparent in the shape of the curves representing gain and phase versus modulation frequency.

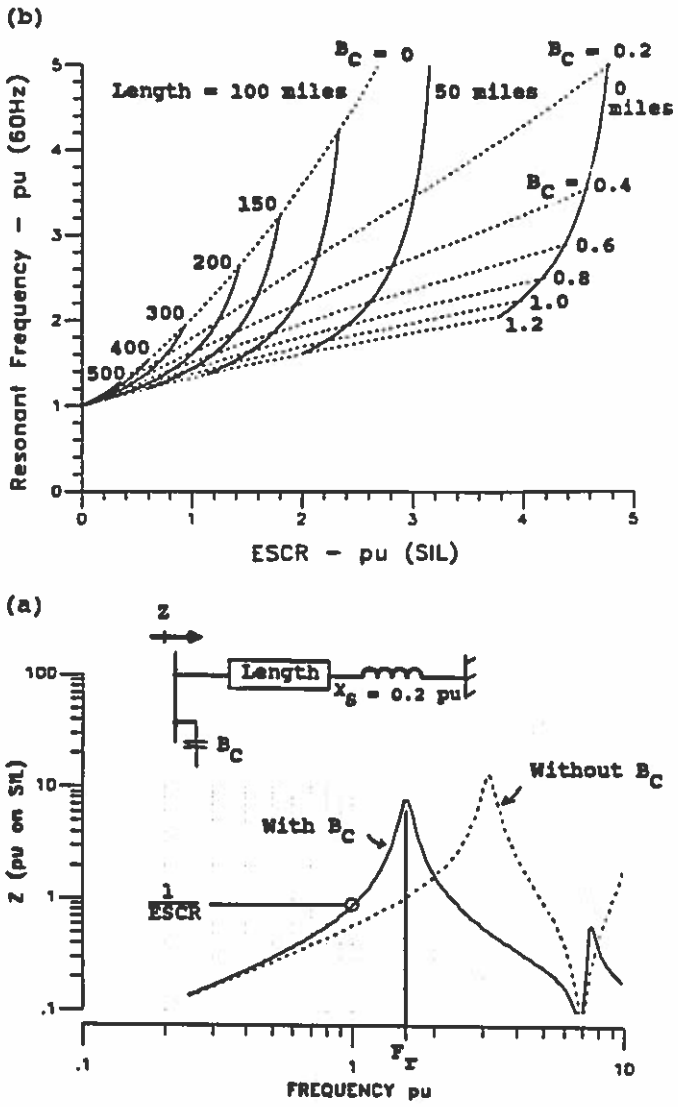

Figure 3.3 Chart Illustrating Relationships of Power System First-Resonant Frequency (F_r) and Effective Short-Circuit Ratio (ESCR) to Parameters of System with Long Transmission Lines.

One important influence of the lower resonant frequency is on the phase lag of the system - note that the phase lag with the 80 Hz system is approximately 100° at 20 Hz, versus only 40° with the 110 Hz system. An additional important factor is the amplification above the steady-state gain due to the resonance. For the 80 Hz system, the response peaks at approximately 20 Hz modulation, with 4.5 db amplification above the steady-state gain (+2.0 db peak - (-2.5 db) steady-state).

The overall effect of the low power-system resonant frequency on SVC voltage control is similar to a second-order control filter inserted within the loop, having a break frequency at approximately the lower sideband of the power system resonance. This is an inherent characteristic of the power system, which aggravates the stability margin of the voltage-control loop.

3.3 Sensitivity to TCR Operating Point

For the SVC voltage control structure assumed for this discussion, the stability margin improves with

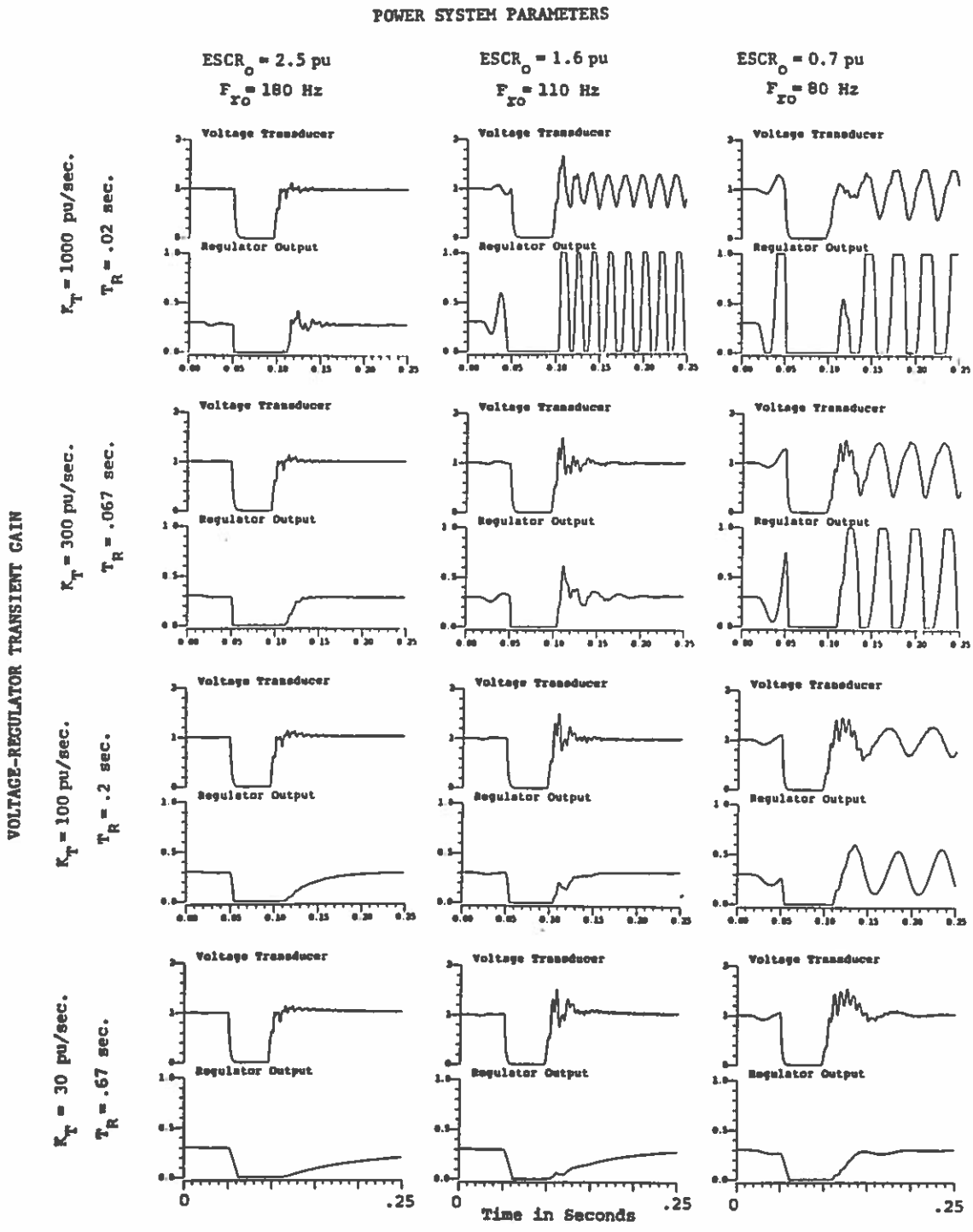

Figure 3.4 Impact of Power System Characteristics on SVC Transient Response with B_{TO} = 0.3 pu.

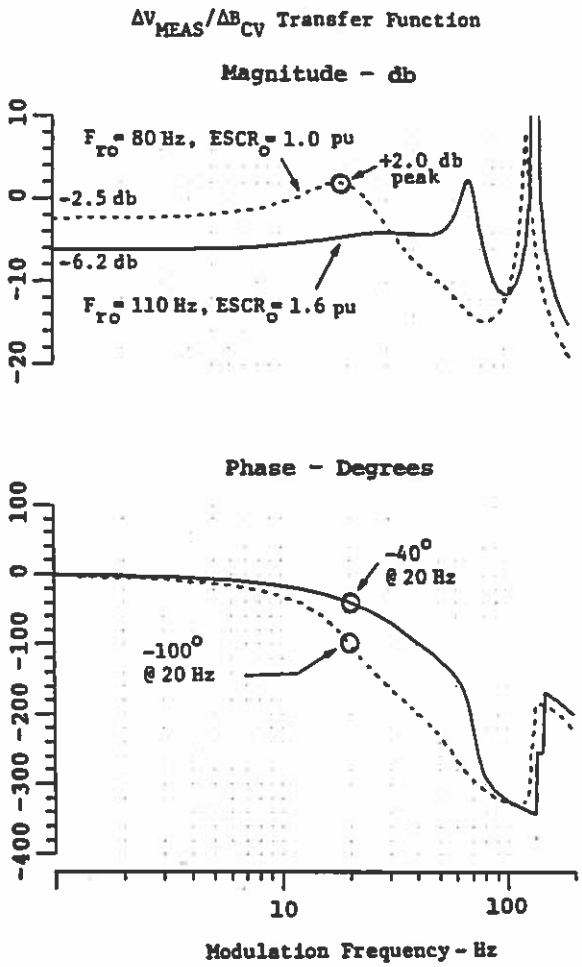

Figure 3.5 Impact of Power System Response Characteristics on Voltage-Sensitivity Transfer Function.

higher levels of average TCR conduction. The basic reason for this effect is that the average operating point of the TCR can be considered as an inductance in parallel with the remainder of the power system.

In effect, the average TCR conduction (B_{To}) strengthens the system, raising both the ESCR and F_r. While the exact mechanism of this interaction is rather complex [9], the effect can be approximated by including an inductance having a value which provides B_{To} at fundamental frequency. The ESCR governing performance will therefore be higher than the parameter $ESCR_o$ by B_{To}. Expressing both on the same base:

$$ESCR_B = ESCR_o + B_{To} \qquad (3.1)$$

where $ESCR_B$ = ESCR which governs performance for small changes about B_{To}.

B_{To} = Average TCR susceptance at steady-state operating condition.

Similarly, the governing resonant frequency (F_{rB}) will be a function of B_{To}. Both the F_{ro} and $ESCR_o$ parameters are involved in the relationship, which can be approximated by:

$$F_{rB}^2 = [F_{ro}^2 (ESCR_o + B_{To}) + F_{Base}^2 B_{To}]/ESCR_o \qquad (3.2)$$

where F_{rB} = Governing resonant frequency with TCR conduction B_{To}.

F_{Base} = Power system frequency (e.g., 60 Hz).

Figure 3.6 indicates the maximum governing resonant frequency (F_{rl}) due to TCR operation at full conduction, as a function of F_{ro} and $ESCR_o$. Note that the influence of TCR conduction is greatest with the weaker systems, as expected.

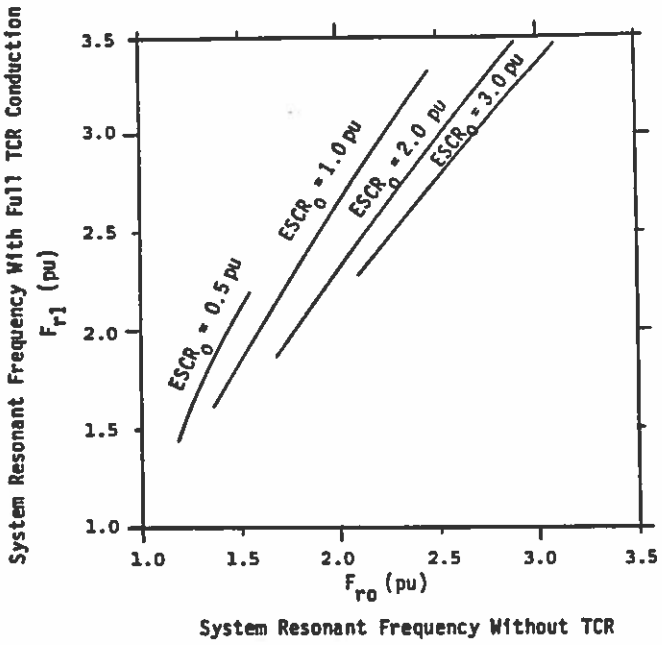

Figure 3.6 Impact of Full TCR Conduction on Effective System Resonant Frequency.

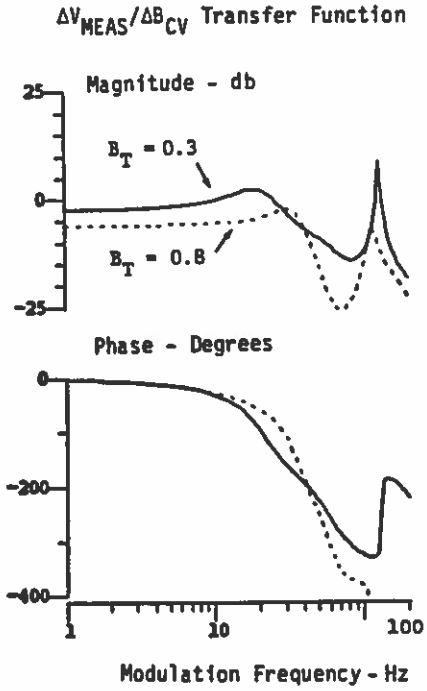

Figure 3.7 Impact of TCR Operating Point on Voltage-Sensitivity Transfer Function.

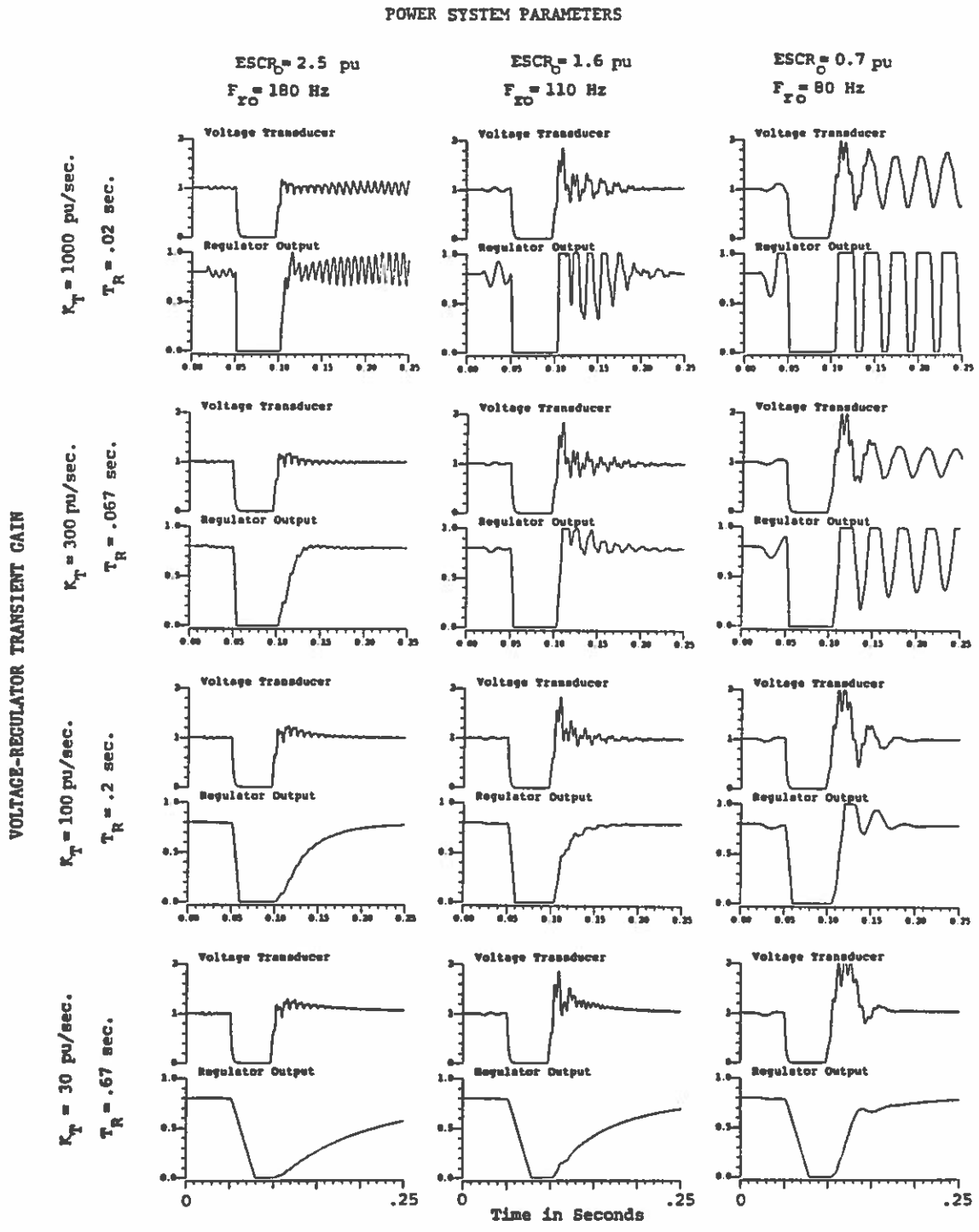

Figure 3.8 Impact of Power System Characteristics on SVC Transient Response with B_{TO} = 0.8 pu.

Simplified analytical relationships based upon the steady-state gains provide a useful basis for understanding the effects. These are developed in Appendix A. The change in effective resonant frequency, however, also causes a change in the dynamic characteristic of the system. An illustration of this phenomenon is given in Figure 3.7, which shows the transfer function from regulator output to voltage magnitude for two different TCR operating points. Comparing Figure 3.7 with Figure 3.5 demonstrates that increasing TCR conduction is similar in effect to strengthening the ac system, including an increase in resonant frequency.

Figure 3.8 indicates the transient response of the system with high TCR average conduction. This figure presents the same cases as Figure 3.4, except with higher source voltage so B_{TO} = 0.8 versus 0.3 pu. Comparing with Figure 3.4 shows the beneficial impact upon stability margin associated with higher TCR conduction. Note that one case, high gain and strongest system, experiences a supersynchronous mode of instability not apparent when operating at low conduction. This is a different phenomenon which is not of practical importance, as it occurs at gains much higher than can be utilized due to consideration of the lower-frequency instability mode.

Some SVC controls include an additional feedback as an inner-loop intended to provide direct control of TCR current from the regulator, rather than controlling only the effective susceptance. Such a control function, if fast enough, can substantially reduce the sensitivity of voltage-regulator stability margin to TCR operating point. However, the net effect is to reduce the stability margin for all operating points to that of the most limiting case without such an inner-loop control function.

3.4 Limitations on Transient Gain

Eigenvalue studies have been performed to determine the transient gain K_{TI} at which the onset of SVC voltage-control instability occurs, for a wide range of power system parameters. Results for operation at B_{TO} = 0.3 pu are presented in Figure 3.9. These results are for a 60 Hz ac system. For a 50 Hz system, both F_{ro} and K_{TI} should be scaled by 50/60.

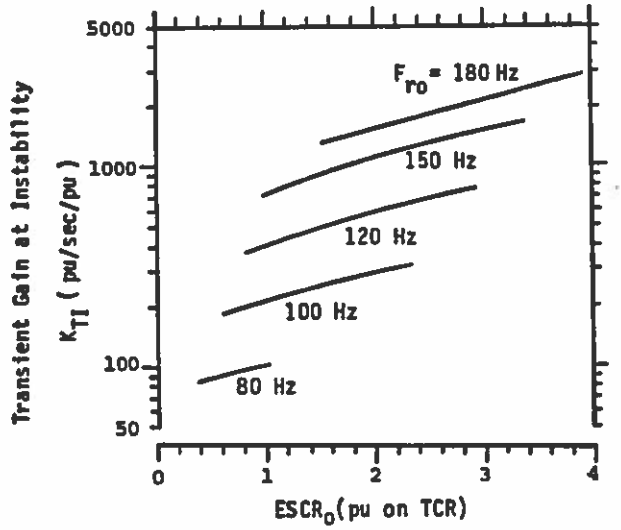

Figure 3.9 Transient Gain at Instability versus Power System Parameters with B_{TO} = 0.3 pu.

The importance of the ac system resonant characteristics is apparent in these results. For a system having the same steady-state gain from regulator output to ac voltage magnitude feedback ($ESCR_O$ = 1.0 pu), but lower resonant frequency (80 Hz versus 110 Hz), the maximum gain is lower by approximately one third (100 versus 300).

For preliminary system studies, a reasonable choice for transient gain would be to use half of the value indicated in Figure 3.9 for the worst ac system contingency. An example follows:

From impedance versus frequency studies, assume that a worst contingency results in $ESCR_O$ = 1.5 pu, F_{ro} = 100 Hz. From Figure 3.9, the transient gain at instability is approximately 250 pu/sec/pu. Using half of this value, with a steady-state gain K_R = 20 pu/pu, the time constant is:

$T_R = K_R/K_T$ = (20 pu/pu) (125 pu/sec/pu) = 0.16 second.

This method should prove helpful for planning studies. Final control parameters for an SVC should be determined during the detailed equipment design studies of the particular application.

3.5 Expected Performance

The initial rate of response to major voltage changes will be dictated by the transient gain. For example, a close-in, three-phase fault will cause the TCR to ramp off at a rate equal to the transient gain. This is illustrated by the cases shown in Figures 3.4 and 3.8.

Post-disturbance return to steady-state will be substantially influenced by the power system characteristics, as discussed in preceding sections and illustrated in Figures 3.4 and 3.8. In general, steady-state will be achieved more rapidly in a weak power system than in a strong system. Note, for example, the three cases at the bottom of Figure 3.8. These cases show the TCR arriving at its final state much quicker for the weaker system than the stronger system. However, the time required for ac voltage to settle out is virtually independent of system strength, provided that the voltage-control loop has a reasonable stability margin.

3.6 Potential Voltage-Control Enhancements

Experience suggests that most applications obtain satisfactory performance with the gains as established in Section 3.4. However, should faster response be needed, options do exist to achieve enhanced performance.

One option is to switch the gain based upon a breaker status signal. This permits higher gains for stronger systems, rather than having the weakest system dictate maximum gain for all conditions [7, 8].

A similar option is to apply an instability detector which continuously monitors the regulator signals, watching for sustained or growing oscillations [7, 8]. Should an instability be detected, the gain is automatically lowered until the oscillations decay. This function also provides for a higher gain with a normal system configuration than would otherwise be dictated by the weakest configuration, as with the gain-switching function; however, an operator-initiated procedure is needed to reinstate the desired gain after the system is reconfigured.

Enhancement of large-disturbance performance can be obtained with some type of nonlinear gain. Experience with bang-bang type of control functions indicates that extreme care must be used in their application. The response is very sensitive to the initiating disturbance, and it is difficult to be sure that all situations have been considered. Should the problem be one-sided, such as placing more emphasis on overvoltages than undervoltages, a gradual change to higher incremental gain on one side of the error signal can generally be safely applied.

Additional compensating networks in the voltage-regulating function have potential for improving the response. These are currently being investigated under the EPRI research project RP2707-1.

3.7 Applications with Multiple Controlled-VAR Devices

The coordination of two performance aspects is required when applying multiple SVC's, or when an SVC is to be placed close to other controlled-VAR devices, such as generators, on the power system:

1. Maximize VAR-sharing between all devices, especially for transient response to major disturbances.

2. Prevent oscillations involving VAR interchanges between devices.

Experience to-date suggests that the VAR-sharing function is the primary concern. No evidence of VAR interchange oscillations has been observed in a number of such studies with which the authors are familiar. However, there have been instances observed during planning studies where an SVC located close to a generator caused the exciter to back off rapidly following a fault, thereby indicating an SVC size larger than necessary to stabilize the system.

Appropriate sharing should be ensured during planning studies made to determine SVC size. Artificial means may be needed to ensure sharing in the study, such as forcing voltage-reference signals. Should such means be needed in the study, then a similar type of function will likely need to be implemented on the system.

Selecting a gain value for SVC's in a multi-SVC application can be based upon the methods indicated in Section 3.4. However, the combined effect of all SVC's acting together must be considered. When performing the impedance versus frequency study for each SVC, the filters, capacitors, and transformers of all other SVC's should be on the system. In addition, the gain of each SVC voltage regulator should be reduced by approximately the ratio of the local SVC rating to the rating of other SVC's on the system which have significant influence on the local voltage.

4. DAMPING POWER SYSTEM SWINGS

Application of an SVC to aid damping of power-system swings requires recognition of the complex nature of the power system. Many modes of electromechanical oscillation, or power-swing modes, exist in large systems, and their characteristics change with system configuration. Loads have an important influence upon the effectiveness of an SVC to aid swing damping, and change with time during the daily load cycle and following power system disturbances. Random noise, caused by a wide variety of sources on the power system, exists on the signals potentially useful as inputs. This noise is within the bandwidth of power swings and hence careful control design is important to avoid excessive response to such noise. Finally, the primary reason for applying the SVC may be for other than damping power swings, and the damping control must be designed so as not to detract from this primary purpose.

These considerations must be thought through when planning such an application. The concepts presented in this paper can serve to guide planning studies to determine the potential benefit of an SVC damping-control modulation function. Such studies should begin assuming a simple, linear modulation control function. A linear modulation function has an advantage of being able to damp several power-swing modes simultaneously, and the performance of such a control in the varying power system environment is relatively independent of particular types of disturbances. As studies progress, the benefits of discrete nonlinear action, such as bang-bang control [10], may become apparent for some events; however, additional extensive studies must then be performed to insure against potentially unfavorable action for other system disturbances.

The location of an SVC strongly affects controllability of the swing modes, although the optimum location is usually obvious - in the middle of the transmission paths between areas, where voltage swings are greatest without the SVC.

There exist many possibilities for input signals upon which to base a damping-control modulation function. Several criteria must be applied in selecting an input signal or a set of input signals appropriate for the particular application. The signal must, of course, be responsive to the swing modes to be damped - this is termed "observability" in control jargon. A local signal is preferred to a communicated signal, since communications add time-delays, and more important, unreliability. The modulation control should provide a positive contribution to damping for any power system operating condition, i.e., the control should be "robust." Local instabilities must be avoided, which can arise when using a measured signal which is directly sensitive to the SVC output. Interaction with other controlled devices on the system will depend on the selected input signal, and should be considered. Finally, the sensitivity to various types of system noise will be different for a given damping contribution achieved with different input signals. With so many considerations, an optimum design might incorporate several input signals.

This paper provides results obtained to-date in the EPRI RP2707-1 research project. These results provide a basis from which many of the important considerations can be evaluated. The characteristics of the application are presented in the context of treating each mode of power system swing independently. This approach provides for understanding the basic issues underlying the application of SVC devices to aid damping in a complex, multi-machine power system.

4.1 Analytical Method - Modal Approach

The forces which influence the modes of machine oscillations in a power system can be conceptually split into synchronizing and damping components of torque. The synchronizing component holds the machines together and is important for system transient stability following large disturbances. For small disturbances, the synchronizing component determines the frequency of oscillations. The damping component determines the decay of the transients and is important for system stability following recovery from the initial swing.

The impact of the synchronizing and damping components of torque on each electromechanical mode of oscillation in a multi-machine system can be determined by decomposing the system variables into their modal components. Figure 4.1 is a block diagram representation of the damping and synchronizing components for the i-th mode of oscillation. For each mode of interest, one can derive such a block diagram. The total system response will consist of the sum of all modal responses.

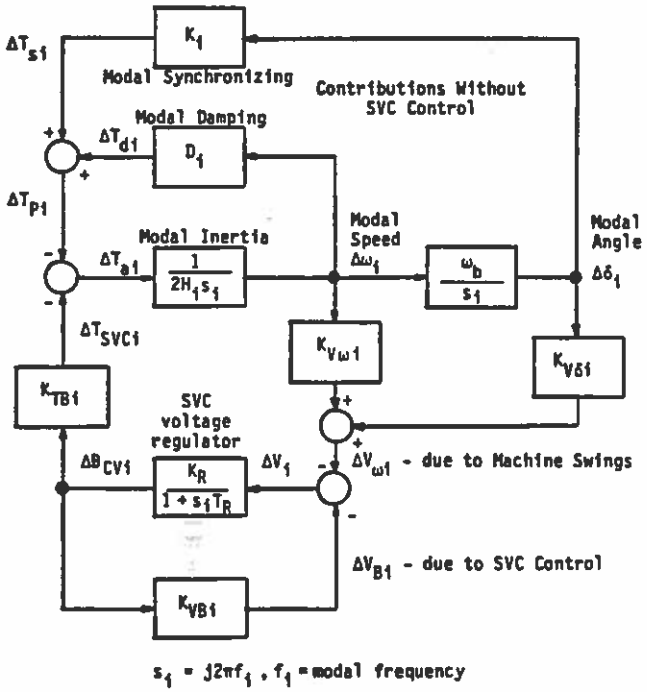

Figure 4.1 Block Diagram Representation of Modal Synchronizing and Damping Torques for Power-Swing Mode "i", Showing SVC Voltage-Control Contribution.

The symbol H_i represents the modal inertia and δ_i and ω_i represent the modal angle and speed of the i-th mode, respectively. The synchronizing torque

$$\Delta T_{si} = K_i * \Delta\delta_i \qquad (4.1)$$

is due primarily to the system transmission interconnections and the voltage-regulating actions of generator excitation systems and other continuously-acting voltage-controlling devices on the power system. The damping torque

$$\Delta T_{di} = D_i * \Delta\omega_i \qquad (4.2)$$

is due primarily to the actions of power system stabilizers on the generator exciters, loads, and, to a lesser degree, turbine-governors.

For the purpose of analyzing the effect of SVC control action on the swing mode, the torque contribution of the SVC is conceptually separated in Figure 4.1 from those due to other influences. The SVC is equipped with a voltage regulator which provides primarily synchronizing torque. The transfer functions K_{TBi} and K_{VBi} represent the sensitivities of modal torque and SVC voltage, respectively, with respect to SVC control action. The transfer functions $K_{V\omega i}$ and $K_{V\delta i}$ represent sensitivities of the SVC voltage with respect to modal speed and angle, respectively. The torque component of ΔT_{SVCi} which is in phase with the modal angle is then the synchronizing contribution of the SVC, while that in phase with the modal speed is the damping contribution.

In general, the damping torque contribution from an SVC with the voltage regulator alone is small. For additional damping contribution, a supplementary control function is necessary. To aid understanding of the application of such a supplementary control, the system is reduced to the simplified block diagram illustrated in Figure 4.2. In this representation, the total transfer function from modal speed to modal torque, via SVC control, is split into two paths, with and without the supplementary control function. The supplementary control function utilizes an input signal "x" to create a modulation signal "V_{MOD}", and is represented by the symbol "$SVSTAB_x$".

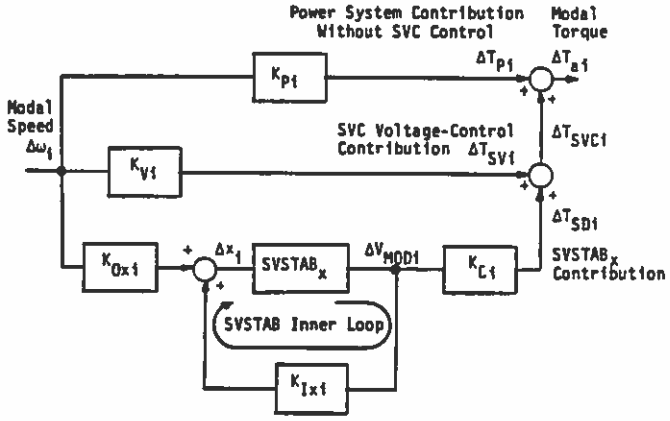

Figure 4.2 Consolidated Block Diagram Illustrating SVC Control Contributions to Speed-to-Torque Transfer Function for ith Power-Swing Mode.

The path involving only voltage control, represented by the symbol K_{Vi}, provides primarily a synchronizing contribution; hence K_{Vi} has a phase angle near -90°. The path involving the supplementary control involves three separate characteristics of the power system plus the SVC voltage regulator. These involve the sensitivity of the input signal to the modal speed K_{Oxi}, the sensitivity of modal torque to the modulation signal K_{Ci}, and the sensitivity of the input signal to the modulation signal K_{Ixi}. Note that the latter sensitivity creates an "inner loop" with the supplementary control function.

Each of these characteristics are discussed in the subsequent sections, illustrating the concepts important for implementing such a supplementary damping control. The relationships of these characteristics to other parameters are given in Appendix B.

4.2 Ability of SVC to Influence Power Swings - Controllability

The sensitivity of modal torque to SVC control modulation, K_{Ci} of Figure 4.2, denotes the ability of the SVC to control the electrical torque of the i-th power-swing mode for a given situation, and hence is termed the "controllability constant." Although strict interpretation of the quantity K_{Ci} defined in Section 4.1 implies that it is a complex variable, the imaginary portion is generally small compared with the real part. Therefore, in subsequent discussions in

this paper, it will be approximated as a scalar to illustrate the important concepts.

In this section, the variations of controllability with important system parameters and operating conditions will be illustrated.

Swing-Mode Controllability in a Two-Area System

The power system representation in Figure 4.3 is used to illustrate an interconnected system of two areas of similar size. Each area is represented by an aggregate machine with an equivalent excitation system, including a power system stabilizer and a speed governor representative of a large area. Each area is assumed to generate at 1 pu power, most of which is consumed by the local loads. An SVC is located between the two areas to improve the power transfer capability between the areas. With the SVC providing voltage support, the inter-area mode of oscillation is near 0.5 Hz. The SVC voltage regulator settings are K_R = 20 pu/pu, T_R = 0.2 second, on a total controllable susceptance rated at 15% of an area. The net capacitance of the SVC is selected for each power transfer to maintain rated voltage at Bus 2.

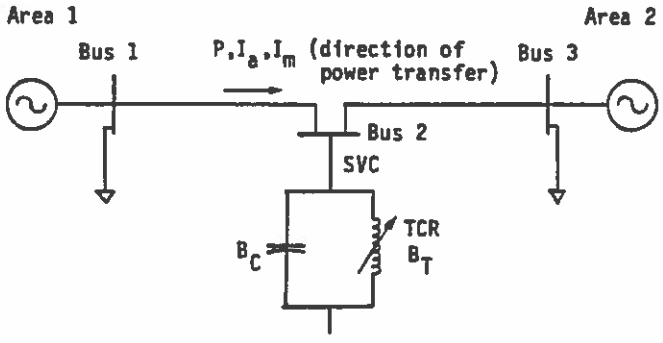

Line Data

From	To	R	X	B
Bus 1	Bus 3	1.0 pu	10.0 pu	0.2 pu

Figure 4.3 Two-Area System Model.

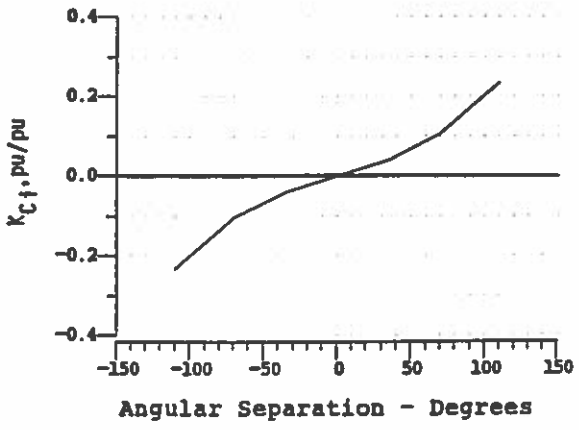

Figure 4.4 Controllability K_{C1} as Function of Intertie Power Transfer, 2-Area System.

Figure 4.4 shows the variation of the controllability constant as a function of the power transfer with the SVC located midway between the two areas. The power transfer is measured as the angular separation between the two areas. A positive angle of separation means that Area 1 is exporting to Area 2. The power transfer between the two areas is approximately 0.16 pu at 110° separation (with 55° across each controlled voltage bus). At zero separation angle, that is, no power transfer, K_{C1} is zero, implying that the SVC has no impact on the electrical torque.

This demonstrates that the SVC becomes more effective for controlling power swings at higher levels of power transfer, which is good since this trend coincides with the expected need for additional damping. However, the sign change with direction of power flow is an important characteristic to account for when designing a damping control function.

Figure 4.5 shows the impact of the SVC location and the area load characteristics on the controllability. The independent axis of Figure 4.5 denotes the relative location of the SVC bus from the exporting area in terms of impedance between areas. The curves in Figure 4.5 are obtained from power transfer conditions of Area 1 exporting, with the larger angular difference between the SVC bus and an area bus being 35°; thus power transfer reduces as the SVC location moves away from the center. Three curves are shown representing load types of constant power, constant-current, and constant impedance for the active power component of the loads. Loads in both areas are of the same type.

As intuition might suggest, the SVC exerts maximum control over power swings when located midway between areas. Also, the effect of load type is greatest when the load is closest to the SVC. When the SVC is located near the receiving end, the power-swing controllability increases as loads tend toward constant power type. This is beneficial, since constant-power loads tend to decrease the system damping. However, if the load tends toward constant impedance, the impact of control modulation may reverse sign - possibly resulting in a negative-damping contribution.

Thus, the inherent ability of the SVC to enhance power-swing damping is best if the SVC is located near the midpoint of the intertie. The effect of locating the SVC towards either the receiving or sending end depends greatly upon the voltage-sensitivity of the loads, as defined by the data presented in Figure 4.5.

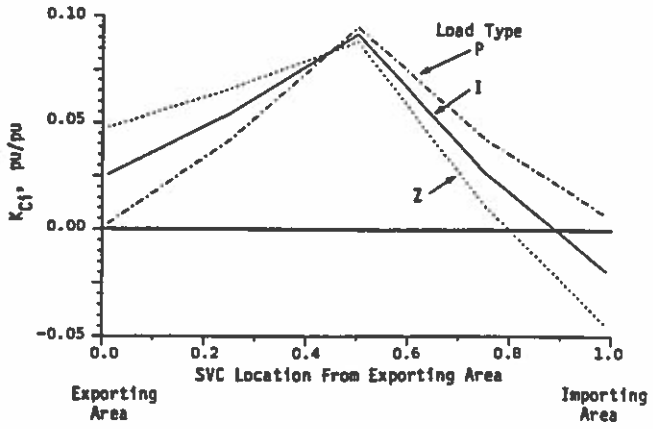

Figure 4.5 Controllability K_{C1} as Function of SVC Location and Load Types in 2-Area System.

Swing-Mode Controllability in a Three-Area System

The basic concepts of controllability variations as a function of power transfer, location, and load type apply also to multi-machine environments. As an example, the two-area system previously used to illustrate the basic concepts is expanded to a 3-area system by splitting one of the areas as indicated in Figure 4.6. This system has two modes of oscillation, at approximately 0.4 Hz and 0.9 Hz. The lower-frequency mode involves primarily Area 1 swinging against Areas 2 and 3, while the higher-frequency mode involves primarily Area 2 swinging against Area 3.

With the SVC located midway along the intertie (bus 1 to 5), the controllability constants for the two modes vary with intertie power transfer as illustrated in Figure 4.7. In this case, the angular separation is between bus 1 and bus 2, and the relative flows to Areas 2 and 3 are adjusted to have the same angles at buses 2 and 3. A positive angle means that Area 1 is exporting to Areas 2 and 3.

Note that the trend for each mode is similar to that for the single mode of a two-area system. The controllability is greatest at highest power transfer, and changes sign at some intermediate level of power transfer. The controllability of the higher-frequency mode is lower than that of the lower-frequency mode due to the location of the SVC relative to the respective mode shapes.

Locating the SVC closer to the midpoint of the higher-frequency mode will increase the controllability of that mode. However, in this case the midpoints of the two modes are at different locations on the power system so increasing the controllability of one mode may decrease the controllability of the second mode. Figure 4.8 illustrates the effect of moving the SVC to bus 5 - at the end of the intertie closest to the areas mostly involved with the higher mode. The controllability of the 0.9 Hz mode increases while that of the 0.4 Hz mode decreases.

4.3 Input Signal Selection

Several factors must be considered when selecting an input signal for a power-swing damping control function on an SVC. These are summarized in the introductory portion of Section 4, consisting of the following points:

1. Responsiveness to swing modes ("observability").
2. Robustness with varying power-system operating conditions, i.e., always making a positive-damping contribution.
3. Local versus remote.
4. Impact on first-swing stability, and subsequent voltage deviations.
5. Potential for localized control instability.
6. Potential for interaction with other controlled devices on power system.
7. Potential for excessive response to random noise.

This section provides a discussion of observability, robustness, and localized control instability potential for selected input signals. The impact on first-swing stability, synchronizing, and voltage deviations will be briefly discussed. The potential for interactions with other controlled devices and for

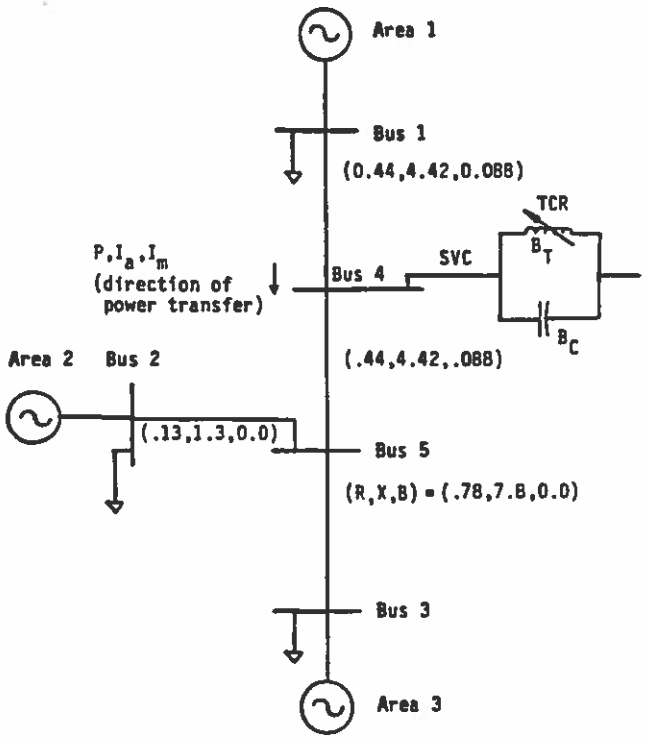

Figure 4.6 3-Area System Model.

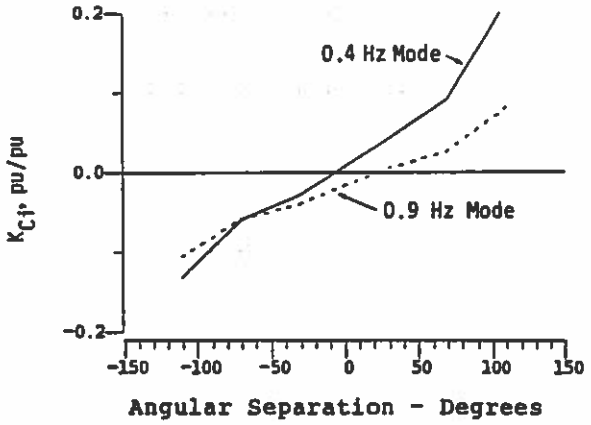

Figure 4.7 Controllability K_{C1} as Function of Intertie Power Transfer, 3-Area System, SVC Midway on Intertie.

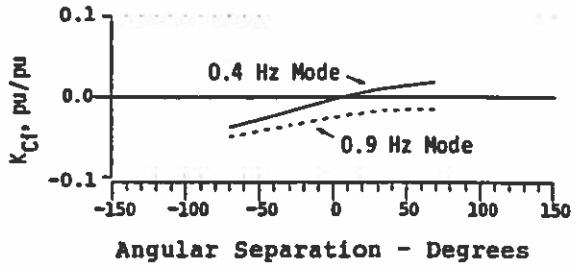

Figure 4.8 Controllability K_{C1} as Function of Intertie Power Transfer, 3-Area System, SVC at Bus 5.

excessive response to random noise are currently being investigated in the EPRI RP2707-1 project, and will be reported at a later date.

Input Signal Choices

At least three basic types of signals may be used as inputs to a damping control function:

1. Frequency of an ac voltage.

2. Current or power flow on major lines.

3. Voltage magnitude.

Frequency types are directly related to the actual speed changes of the generators. However, these are most sensitive to the swings when measured close to the generators, and are usually insensitive when measured in the middle of transmission paths where an SVC is likely to be located. Current flows are directly related to angular differences between areas, but require inputs from CT's representing flows on important lines. In some cases, it may not be clear on which line or lines current should be measured. Voltage magnitude is strongly related to angular differences between areas, as are current measurements, but is also strongly influenced by the action of the SVC controls.

These basic characteristics are quantified in the following discussion.

Desirable Characteristics

From the controller design considerations, a desirable input signal should have the following characteristics:

1. The observability K_{Oxi} should have large values, especially at high power transfer levels, to impact on T_{SVC}.

2. A desired level of damping should be achieved by using a controller $SVSTAB_x$ that results in a low inner-loop gain, such that the internal dynamics of the SVC would not be oscillatory or substantially affect damping performance.

3. A positive contribution should be made to damping over a wide range of operating conditions, including reversals of power transfer directions. If the damping contribution changes sign, then an adaptive controller which senses the system operating condition and adjusts the controls needs to be used. Designing such an adaptive scheme to ensure robustness on a large, time-varying system could be quite difficult.

Characteristics of Selected Signals

The relative merits of a representative set of locally measurable signals are evaluated here in terms of the characteristics discussed above. The signals considered to illustrate the basic concepts are:

- f - SVC bus frequency
- V - SVC bus voltage
- P - Active power transfer
- I_a - Active component of line current
- I_m - Line current magnitude

The evaluations will be made for the two-area system, with the SVC located midway between areas. The active power transfer and active line current are measured so that they are positive for power transfer from Area 1 to Area 2. The signals P, I_a and I_m are measured on the line connected to Area 1. Similar conclusions are reached for these signals measured on the line connected to Area 2.

Figure 4.9 shows the observability and inner-loop characteristics of the selected input signals, as a function of power transfer and intertie impedance.

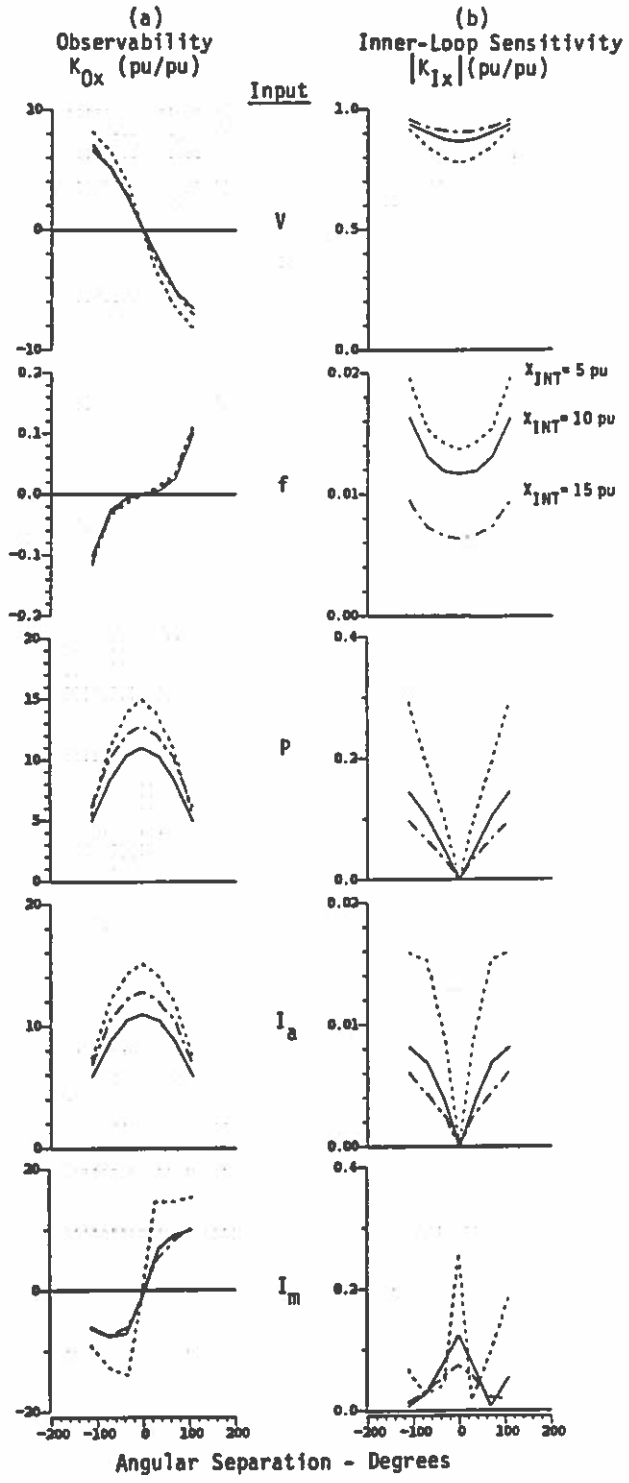

Figure 4.9 Observability and Inner-Loop Sensitivity of Various Input Signals versus Intertie Power Transfer and Impedance.

Column (a) indicates the observability constant K_{Oxi}, for which the major components of these complex variables are plotted to give an indication of sign changes as well as magnitude. Column (b) indicates the magnitude of the inner-loop constant K_{Ixi}. The phase angle of the observability constant is relatively independent of operating condition, except for the sign changes as shown in Figure 4.9a. The phase of the inner-loop characteristic, however, varies substantially with operating condition, including changes approaching 180° for some signals.

The following points are significant to note:

1. For both voltage and current-magnitude signals, the sign of the observability constant changes with power transfer direction, and the magnitude of the observability increases with the amount of power transfer.

2. For both power and active current flow signals, the magnitude of the observability decreases with the amount of power transfer, and the sign is independent of power transfer direction.

3. For the frequency signal, the observability is low, being less than 10% of the modal speed for all cases. The sign of the observability changes with power transfer direction in this particular case, due to the SVC being located precisely in the center of the transmission path between identical areas. Were the SVC located closer to one end or if the areas were not identical, the sign of the observability would be very sensitive to the particular situation.

4. The inner-loop magnitude is very sensitive to operating condition. Of particular importance are the conditions for maximum inner-loop response. For voltage input, this occurs at the maximum shunt capacitive compensation on the weakest transmission configuration. For current-magnitude input, this occurs at minimum shunt capacitive compensation with the strongest transmission system configuration. Note that shunt capacitive compensation is the actual contributing parameter to these inner-loop gains, while the curves of Figure 4.9 show the relation to power flow; shunt compensation must increase to support higher power transfer.

SVSTAB Transfer Function Requirements

Referring to Figure 4.2, it is seen that the effect of the SVSTAB control function on power-swing damping is proportional to the product of the controllability and the observability characteristics. Provided the inner loop gain is low, the effect is also proportional to the SVSTAB transfer function.

Since the inner-loop characteristic of the system varies substantially in both phase and gain with power system operating condition, it is important to design the SVSTAB function such that the inner loop does not have a significant effect on the performance. This implies that the total inner loop gain must be significantly less than unity for all power system conditions:

$$|SVSTAB_x| \quad |K_{Ixi-max}| \ll 1 \tag{4.3}$$

where $|K_{Ixi-max}|$ = Maximum magnitude of K_{Ixi} for all power system conditions.

For a specified inner-loop gain margin, the maximum gain of the SVSTAB function at the swing-mode frequency can be defined in terms of $K_{Ixi-max}$. In addition, the phase shift of SVSTAB needed to provide a purely positive-damping contribution can be defined for a specific power-system operating condition in terms of the controllability and observability constants. Equations 4.4 and 4.5 define these relationships for a reference power-system operating condition, and provide a good starting point for synthesizing a damping-control function:

$$SVDMAX_{xi} = e^{j\theta_{Rxi}}/GM_{IL}|K_{Ixi-max}| \tag{4.4}$$

$$\theta_{Rxi} = -\text{angle}\{K_{CiR}\ K_{DxiR}\} \tag{4.5}$$

where $SVDMAX_{xi}$ = Frequency response of $SVSTAB_x$ transfer function at s_i for maximum damping contribution to mode "i" using input signal "x", with desired inner-loop gain margin.

s_i = $j2\pi f_i$

f_i = Frequency of ith power-swing mode.

θ_{Rxi} = Reference angle, needed for $SVSTAB_x$ to provide pure damping for a reference case with negligible inner-loop effect.

GM_{IL} = Desired minimum inner-loop gain margin (typically 10 db or more).

K_{CiR}, K_{OxiR} = Controllability, Observability constants for the reference case.

Damping Contributions With Selected Signals

The maximum damping attainable varies with the selected input signal, as does the relationship of damping contribution to power system operating condition. For the purpose of comparing the selected input signals, we define a maximum-attainable damping parameter for each. This parameter approximates the damping contribution associated with using $SVDMAX_{xi}$ defined in Equation 4.4 in other power system conditions:

$$DMAX_{xi} = \text{Real}\{K_{Ci}\ K_{Oxi}\ SVDMAX_{xi}\} \tag{4.6}$$

where $DMAX_{xi}$ = Maximum-attainable damping contribution of $SVDMAX_{xi}$ to swing-mode "i."

Plots of this maximum-attainable damping contribution parameter as a function of power transfer for the two-area system are provided in Figure 4.10. Operation at 70° separation between areas is taken as the reference case, and an inner-loop gain margin of 10 db is used. These plots illustrate the following significant points:

1. Use of active current permits greater damping to be attained than use of other signals, due to low inner-loop sensitivity.

2. Use of voltage is significantly constrained by the inner-loop consideration; this signal is so sensitive to SVC control action that the effect of the modulation masks the power swing.

3. Use of power or active current results in a damping contribution which changes sign as a function of operating condition, necessitating adaptive control to alter the sign of the modulation control as a function of power transfer direction.

4. Use of current-magnitude enables substantial damping to be attained, with a positive contribution for all operating conditions.

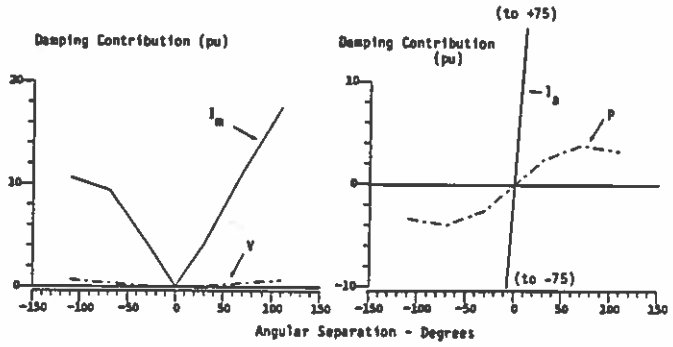

Figure 4.10 Maximum SVSTAB Damping Contributions with 10 db Inner-Loop Gain Margin.

Thus, the choice of input signal is important to the design of an SVC control function to aid power-swing damping. Low sensitivity to SVC control action is desired, as well as an inherent adaptivity characteristic to compensate for changes in the sign of the controllability. For this two-area example, the current-magnitude signal possesses these qualities.

4.4 Damping Controller Design

A set of guidelines is proposed here to synthesize a simple damping controller. These are based upon the foregoing discussions and experience with generator exciter power system stabilizers [11].

1. Select phase shift at dominant swing frequency for mostly positive damping contribution. Any deviation from the phase shift needed for pure damping to be in a direction to enhance synchronizing; e.g., the actual phase shift should lag the "pure-damping" phase shift.

2. Select gain at dominant swing frequency for desired damping contribution at some heavy-load condition, but limited to ensure at least 10db of gain margin for the inner loop in the most constraining system configuration.

Table 4.1 provides the gain and phase data for damping controllers designed for the two-area system using these guidelines, with each of the selected input signals. The desired damping contribution for each input signal was chosen such that the overall system damping was the same with a 70° angle between areas as with no intertie power transfer. Note that the desired damping is achievable for this case with the line-flow input signals, but not with the voltage magnitude or frequency inputs.

Table 4.1

Damping Controller Characteristics at 0.5 Hz
For 2-Area Power System, SVC Midway on Intertie

Input Signal	Pure-Damping Phase Shift	Gain (pu/pu) for Desired Damping	Gain (pu/pu) for Inner-Loop Constraint	Inner Loop Worst-Case Gain Margin
Voltage	-121°	2.5*	0.35	10 db
Frequency	+162°	345*	20	10 db
Power	+93°	1.4	1.4	15 db
I active	+91°	1.5	1.5	39 db
I magnitude	+91°	1.5	1.5	22 db

* This gain would achieve desired damping if inner loop gain margin were > 10 db; however, actual inner loop effect would prevent attainment of desired damping even with much higher damping control gain.

Realization of these gain and phase characteristics in a transfer function requires a certain amount of fitting and engineering judgment. A suggested structure for the transfer function includes washout and high-frequency filtering stages, to minimize the response to signals other than those created by the swing modes for which damping is to be provided. However, the response should be consistent over a wide enough frequency range to accommodate changes in swing frequency with system conditions. A simple structure providing these characteristics is illustrated in Figure 4.11. A sample frequency response using constants selected for using line current as an input is shown in Figure 4.12.

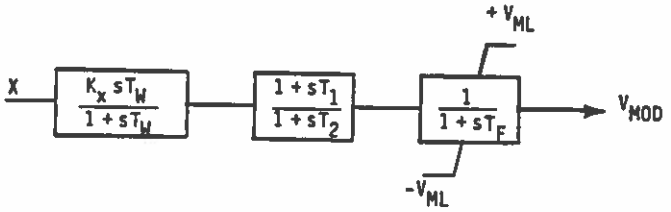

Figure 4.11 Simple $SVSTAB_X$ Structure.

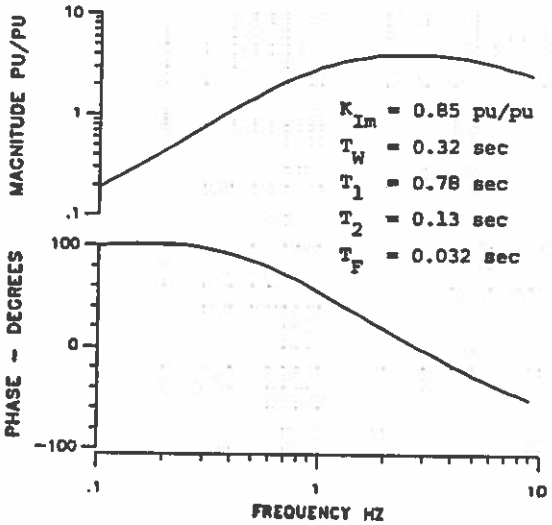

Figure 4.12 Sample Transfer Function of Damping Controller with I_m Input.

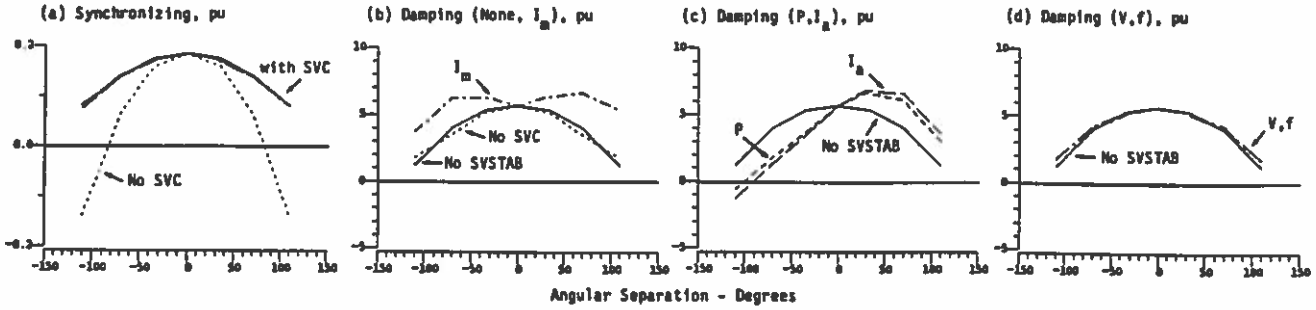

Figure 4.13 Synchronizing and Damping Characteristics of 2-Area 0.5 Hz Swing Mode versus Intertie Power Transfer for Various SVSTAB Input Signals.

4.5 Damping Controller Performance

This section presents results obtained by applying the guidelines of Section 4.4 to synthesize simple damping controllers with each of the selected input signals for SVC's on both the 2-Area and 3-Area systems discussed in this paper.

The following results are for an SVC located midway on the intertie between the areas. The damping and synchronizing characteristics versus power transfer results are obtained assuming the gain and phase of the damping controller determined with the procedure of Section 4.4 are achieved at the swing frequency with 70° separation, area 1 exporting. The time simulations are performed with a damping controller structured as Figure 4.11, with parameters similar to those of Figure 4.12.

Two-Area System

The influence of the SVC with various damping control designs on the synchronizing and damping characteristics of the swing mode are shown in Figure 4.13. Figure 4.13a shows the synchronizing coefficient with and without the SVC. The curves labeled as being with the SVC represent both simple voltage control and having each of the damping controllers applied in turn.

Note that the system cannot remain synchronized beyond 90° separation without the SVC, as indicated by the negative synchronizing coefficient for these cases. With the SVC, positive synchronizing is maintained beyond 90°. The contribution from the SVC increases as the angular separation increases, resulting in a more uniform synchronizing effect over the range of power transfer. Addition of the damping controllers does not significantly affect the synchronizing torque, as expected since the phase is determined for pure damping contribution at one of the operating points.

The SVC without the damping controller does not contribute much damping torque, as indicated in Figure 4.13b by the small difference between curves labeled NO SVC and NO SVSTAB. Also illustrated in Figure 4.13b is the damping contribution obtained from using current magnitude as an input. Note that the contribution is positive for all power transfer levels, increasing with the level of power transfer.

Using power or the active component of line current as an input yields the damping contribution shown in Figure 4.13c. Note that the damping contribution changes sign as the direction of power transfer reverses.

Very little damping enhancement is possible using voltage magnitude or frequency inputs, as shown in Figure 4.13d.

Responses to a major disturbance are illustrated in Figure 4.14, comparing performance with damping controllers using current magnitude input and power input versus the SVC under voltage regulator control only. Several performance aspects are illustrated in this example.

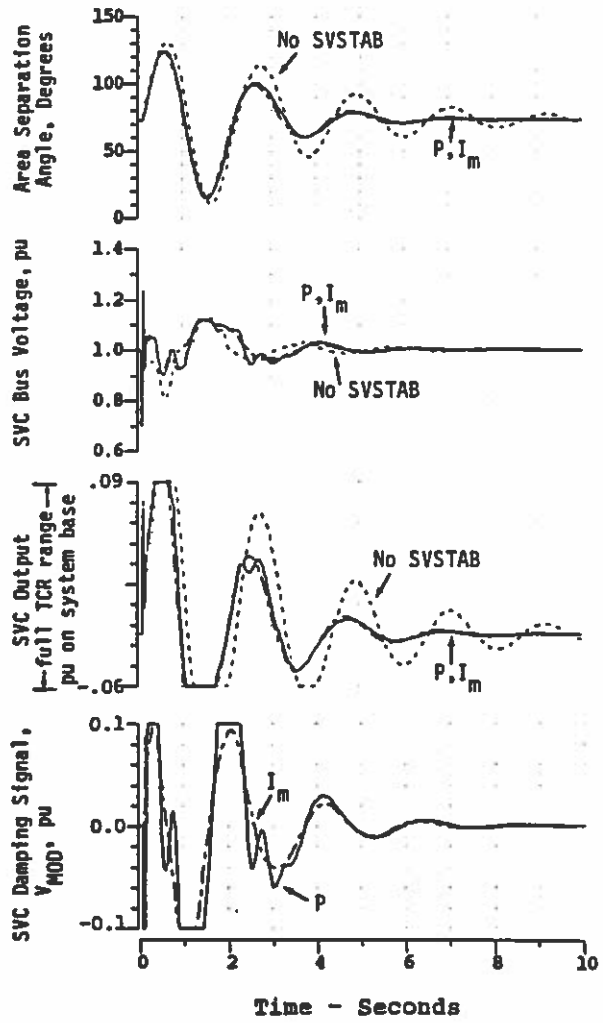

Figure 4.14 Time Simulation of Disturbance in Area 1 of 2-Area System, Area 1 Exporting, with and without SVSTAB. Area 2 is Reference.

1. The damping control function reduces the magnitude of the first swing, both in angle and midpoint voltage. This is due to the more rapid response to the disturbance obtained by sensing a quantity other than voltage.

2. With power input, additional oscillations are apparent on the output of the damping signal, at a frequency higher than the power system swing. This is due to a lower gain margin of the inner loop compared with the current-input design, such that the inner loop dynamics become evident in the response.

The first observation is very important. When a disturbance causes the power system to swing close to its stability limit and the SVC voltage support is crucial, the amount of voltage dip is very sensitive to even small changes in SVC output. These results indicate that addition of a control function intended primarily to aid post-disturbance damping can also serve to enhance first-swing stability.

The second observation indicates that the damping-control gain could be further increased if current magnitude is used, while this case represents the most that can be expected using power flow as an input signal.

Figure 4.15 demonstrates the negative-damping contribution when the direction of power transfer reverses and line power is used as an input signal. This is a simulation of a disturbance with power transfer from Area 2 to Area 1. Note that the damping controller using current magnitude as an input provides positive damping, while the power-input stabilizer is completely out of phase and provides negative damping.

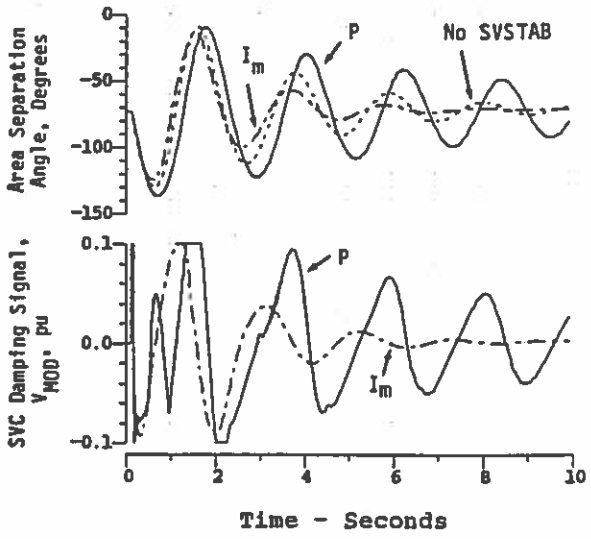

Figure 4.15 Time Simulation of Disturbance in Area 2 of 2-Area System, Area 1 Importing, with and without SVSTAB. Area 2 is Reference.

Three-Area System

Following the suggested design procedure for the three-area system, focusing on the lowest-frequency swing mode, yields damping control designs similar to those for the two-area system.

The influence on the lowest mode of the three-area system is illustrated in Figure 4.16. The relative effect on damping contribution achievable with the various input signals is consistent with the results for the two-area system. The only noticeable difference is that the SVC without a damping control has a greater influence on damping than indicated with the two-area system (Figure 4.16b). Without the SVC, very low damping exists for power transfer from Area 1, even becoming negative for large angles. The most likely reason for this difference compared to the two-area system is the change in location of the loads. Addition of the SVC with a simple voltage control increases the damping for this situation, although it decreases damping for power transfer in the reverse direction.

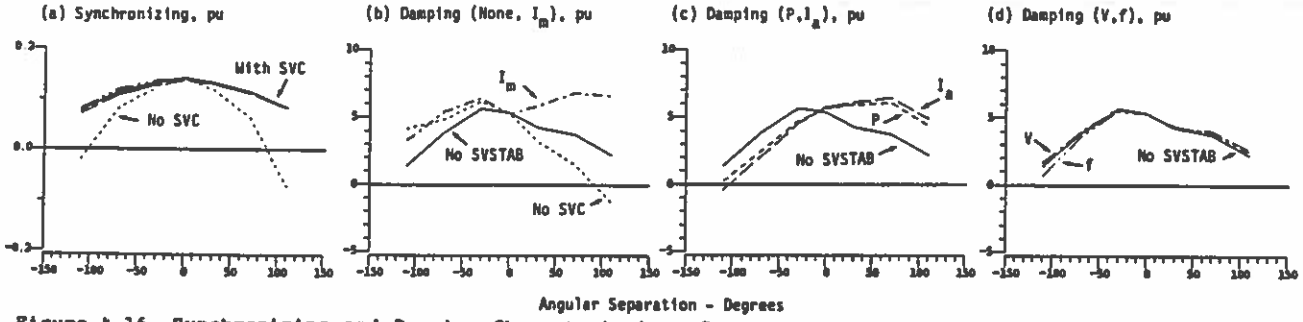

Figure 4.16 Synchronizing and Damping Characteristics of 3-Area 0.4 Hz Swing Mode versus Intertie Power Transfer for Various SVSTAB Input Signals.

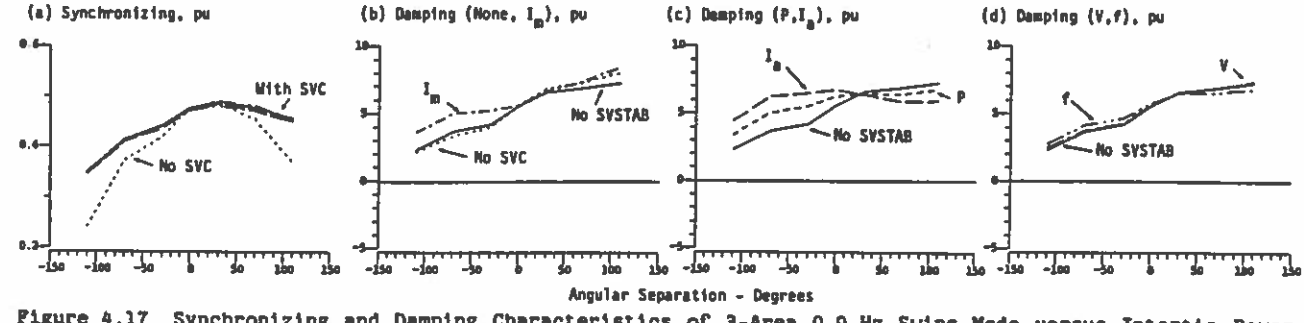

Figure 4.17 Synchronizing and Damping Characteristics of 3-Area 0.9 Hz Swing Mode versus Intertie Power Transfer for Various SVSTAB Input Signals.

The influence on the higher mode is illustrated in Figure 4.17. The relative impacts are generally the same as on the lower mode. Addition of the SVC enhances synchronizing, and use of a damping controller having current magnitude as an input signal provides a positive damping contribution for all intertie power transfer conditions.

One difference is that a damping controller using frequency as an input has greater influence on the higher mode. This is because the SVC is not at the midpoint of this swing mode, and hence the frequency signal contains a greater content of the modal speed. Unfortunately, however, the contribution to damping of the higher mode changes sign with direction of intertie power transfer when using frequency as an input. This effect is because the controllability of the 0.9 Hz mode changes sign at approximately 30° separation (Figure 4.7), while the observability of this mode with frequency input does not change sign.

These observations are further illustrated by the time-domain simulations presented in Figures 4.18 and 4.19. Figure 4.18 illustrates the system response following a disturbance in Area 1, while exporting. The swings of Area 1 angle reflect primarily the lower mode, while Area 2 angle contains some of both modes. Stimulation of the higher mode is shown in Figure 4.19, caused by a disturbance in Area 2. In this case, both modes are stimulated.

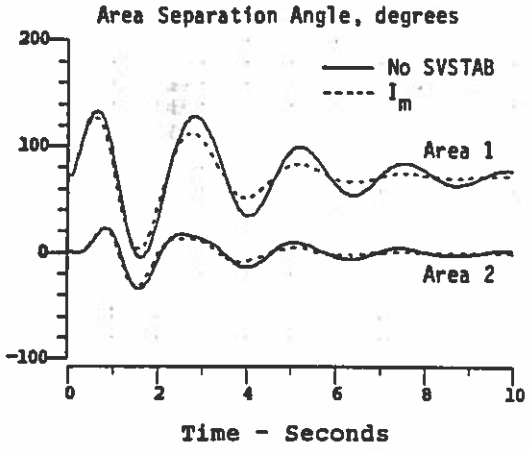

Figure 4.18 Area Swings for Disturbance in Area 1 of 3-Area System, Area 1 Exporting, with and without I_m SVSTAB. Area 3 is Reference.

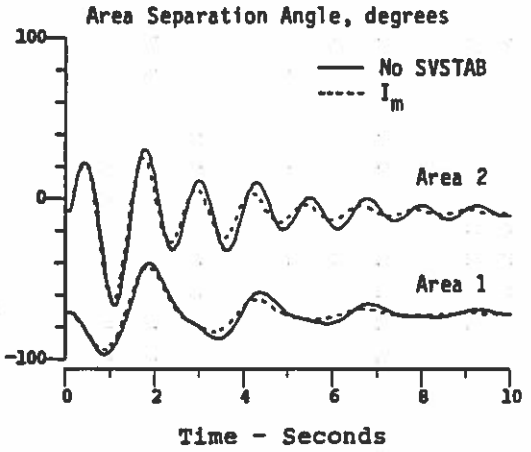

Figure 4.19 Area Swings for Disturbance in Area 2 of 3-Area System, Area 1 Importing, with and without I_m SVSTAB. Area 3 is Reference.

These transient response cases illustrate the benefit of SVC damping control to both modes, even when both exist simultaneously.

5. CONCLUSIONS

This paper presents many insights which should be helpful to engineers studying the potential benefits of SVC application. The critical factors influencing the stability of the voltage regulation function of the SVC are presented, along with guidelines for preliminary selection of gain and time-constant.

Guidelines are also suggested for selecting input signals and transfer function parameters for a simple supplemental SVC control function to enhance power swing damping. While considerable work remains to be done in this area, the concepts presented in this paper should provide a foundation upon which innovative engineers can build to evaluate the potential benefits to their power systems.

6. ACKNOWLEDGMENTS

The results presented in this paper were made possible by the efforts of many individuals, the commitment of the General Electric Company in developing SVC analysis tools since the late 1970's, and the recognition by the Electric Power Research Institute of the potential for enhancing power system performance via application of SVC's. In addition to the authors, the contributors at General Electric include Dan Baker, Jack Cutler, Hamid Elahi, Ron Hauth, Dave Kankam, Stan Miske, Bob Moran, Nick Miller, Farhad Nozari, Dick Piwko, Juan Sanchez-Gasca, and Jim Tice. Stig Nilsson and Harshad Mehta at EPRI recognized the need for research on improving SVC controllability and initiated RP2707-1, which enabled the existing tools and engineering experience to be applied to the benefit of the industry. John Marks of EPRI is currently the project manager of RP2707-1. Discussions with Charlie Concordia and John Hauer (of BPA) have also contributed to the concepts presented in this paper.

7. ANALYTICAL TOOLS

Eigenvalue and other frequency-domain analyses presented in this paper were performed with the MANSTAB/POSSIM/FREQRESP [12] family of computer tools. These tools were developed by General Electric many years ago, and have been validated with other simulation tools and with comparisons to field measurements. Time-domain analyses were performed with POSSIM for the power-swing damping studies, and with the EMTP [13] developed by BPA, for the cycle-by-cycle simulations.

8. REFERENCES

[1] R.L. Hauth, T. Humann, R.J. Newell, "Application of a Static VAR System to Regulate System Voltage in Western Nebraska," IEEE Transactions, Vol. PAS-97, No. 5, September-October 1978, pp. 1955-1964.

[2] IEEE Tutorial Course Text: Power Electronics Application in Power Systems, 78 EH0135-4-PWR, 1978.

[3] EPRI Proceedings: Transmission Static VAR Systems Seminar, Special Report EL-1047-SR, WS-78-108, April 1979.

[4] International Symposium on Controlled Reactive Compensation, IREQ, Varennes, Quebec, September 1979.

[5] "Reactive Power Control in Electric Power Systems," T.J.E. Miller, Editor, John Wiley & Sons, New York, 1982.

[6] "Bibliography of Static VAR Compensators," IEEE PES Substations Committee, WG 79.2, IEEE PAS Transactions, Vol. PAS-102, No. 12, pp. 3744-3752, December 1983.

[7] "Static Compensators for Reactive Power Control," Canadian Electrical Association, Cantext Publications, Winnipeg, 1984.

[8] "Static VAR Compensation," I.A. Erinmez, Chairman, CIGRE GW 38-01, Task Force No.2 on SVC, CIGRE, Paris, 1986.

[9] L.J. Bohmann, R.H. Lasseter, "Equivalent Circuit for Frequency Response of a Static VAR Compensator," IEEE Transactions, Vol. PWRS-1, No. 4, November 1986, pp. 68-74.

[10] A.E. Hammad, "Analysis of Power System Stability Enhancement by Static VAR Compensators," IEEE Transactions, Vol. PWRS-1, No. 4, November 1986, pp. 222-227.

[11] E.V. Larsen, D.A. Swann, "Applying Power System Stabilizers, ... Parts I-III," IEEE Transactions, Vol. PAS-100 No. 6, June 1981, pp. 3017-3046.

[12] E.V. Larsen, W.W. Price, "MANSTAB/POSSIM Power System Dynamic Analysis Programs - A New Approach Combining Nonlinear Simulation and Linearized State-Space/Frequency Domain Capabilities," IEEE PICA Proceedings, 1977, pp. 350-359.

[13] ElectroMagnetic Transients Program Rule Book, Bonneville Power Administration, Portland, Oregon, June 1984.

Appendix A

Simplified Relationships Between System Strength, Average TCR Operating Points, and SVC Voltage Control-Loop Gain

(a) TCR Only

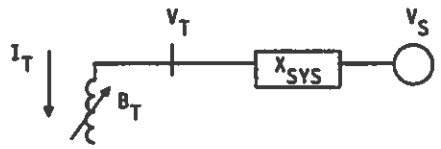

Assuming that V_S is a constant voltage source in the simplified representation of the system as viewed from the TCR, a perturbation of the SVC voltage V_T due to a perturbation of the current I_T is related as

$$\Delta V_T = - X_{SYS}\ \Delta I_T. \qquad (A.1)$$

Within the TCR, the current, voltage, and B_T perturbations are related by

$$\Delta I_T = \Delta V_T\ B_{To} + \Delta B_T\ V_{To}. \qquad (A.2)$$

Substituting ΔI_T from (A.2) into (A.1) yields the SVC voltage control loop gain

$$\frac{\Delta V_T}{\Delta B_T} = \frac{- V_{To}}{(ESCR + B_{To})} \qquad (A.3)$$

where the effective short circuit ratio is defined as

$$ESCR \triangleq 1/[- \Delta V_T/\Delta I_T] = 1/X_{SYS} \qquad (A.4)$$

(b) Measuring High-Side Voltage

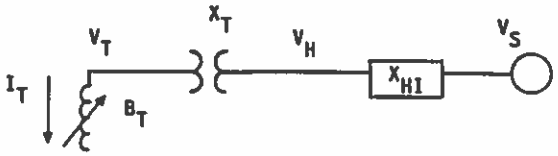

To obtain the SVC high-side voltage control loop gain, the transformer reactance is separated from X_{SYS}. Substituting V_{To} as a function of V_{Ho} into (A.3), the required gain expression is

$$\frac{\Delta V_H}{\Delta B_T} = \frac{- V_{Ho}}{(ESCR + B_{To})} \frac{(1 - X_T\ ESCR)}{(1 + X_T\ B_{To})} \qquad (A.5)$$

Appendix B

This appendix summarizes the relationships between parameters of the power system for modal representation of SVC control action. All terms are defined on Figures 4.1 or 4.2, and are expressed as complex variables evaluated at the "i-th" modal frequency

$$s_i = j\ 2\pi\ f_i \qquad (B.1)$$

where f_i = frequency of ith power-swing mode.

The SVC voltage regulator is involved in all characteristics. The relationships will be given in terms of the closed-loop voltage regulator transfer function at the modal frequency:

$$VLOOP_i = VREG_i\ K_{VBi}/(1 + VREG_i\ K_{VBi}) \qquad (B.2)$$

where $VREG_i$ = Voltage regulator transfer function at modal frequency

$$= K_R/(1 + T_R\ s_i) \qquad (B.3)$$

Typically, the voltage regulating loop will have a bandwidth much higher than the swing mode; hence $VLOOP_i$ will typically be close to unity magnitude, with 5° to 20° of phase lag.

An additional consolidation is made of the speed and angle coefficients from Figure 4.1 to obtain an equivalent, complex transfer function from speed as follows. To define the impact upon a signal "x" due to speed variations, including the angle path:

$$K_{x\delta\omega i} = K_{x\omega i} + K_{x\delta i}\ \omega_b/s_i \qquad (B.4)$$

where ω_b = base system frequency (rad/sec).

The consolidated characteristics of Figure 4.2 are related to the other parameters as follows:

$$K_{Vi} = K_{TBi}\ K_{V\delta\omega i}\ VLOOP_i/K_{VBi} \qquad (B.5)$$

$$K_{Ci} = K_{TBi}\ VLOOP_i/K_{VBi} \qquad (B.6)$$

$$K_{Oxi} = K_{x\delta\omega i} + (K_{xBi}\ K_{V\delta\omega i}\ VLOOP_i/K_{VBi}) \qquad (B.7)$$

$$K_{Ixi} = K_{xBi}\ VLOOP_i/K_{VBi} \qquad (B.8)$$